THE JOURNAL OF PHYSICAL CHEMISTRY B

ARTICLE

pubs.acs.org/JPCB

Evidence for Self-Association of a Miniaturized Version of Agrin from Hydrodynamic and Small-Angle X-ray Scattering Measurements

Trushar R. Patel,*[,†] Tabot M. D. Besong,[‡] Nehal Patel,[§] Markus Meier,[†] Stephen E. Harding,[‡] Donald J. Winzor,[∥] and Jörg Stetefeld[†]

[†]Department of Chemistry, University of Manitoba, Winnipeg, Manitoba, R3T 2N2, Canada

[‡]National Centre for Macromolecular Hydrodynamics, University of Nottingham, Sutton Bonington, LE12 5RD, United Kingdom

[§]Department of Biochemistry and Medical Genetics, University of Manitoba, Winnipeg, Manitoba, R3E 0J9, Canada

[∥]School of Chemistry and Molecular Biosciences, University of Queensland, Brisbane, Queensland 4072, Australia

ABSTRACT: Hydrodynamic studies of miniagrin indicate a molar mass that is 20% larger than the value calculated from the sequence of this genetically engineered protein. Consistent with this finding is the negative sign and also the magnitude of the second virial coefficient obtained from small-angle X-ray scattering measurements. The inference that miniagrin reversibly self-associates is confirmed by a sedimentation equilibrium study that yields an equilibrium constant of 0.24 L/g for a putative monomer−dimer interaction. Finally, Guinier analysis of the small-angle X-ray scattering (SAXS) results yields concentration-dependent values for the radius of gyration that may be described by the monomer−dimer model and respective R_g values of 40 and 105 Å for the monomeric and dimeric miniagrin species. Although intermolecular protein interactions are endemic in the events leading to acetylcholine receptor aggregation by agrin, the matrix proteoglycan of which miniagrin is a miniaturized model, this investigation raises the possibility that agrin may itself self-associate.

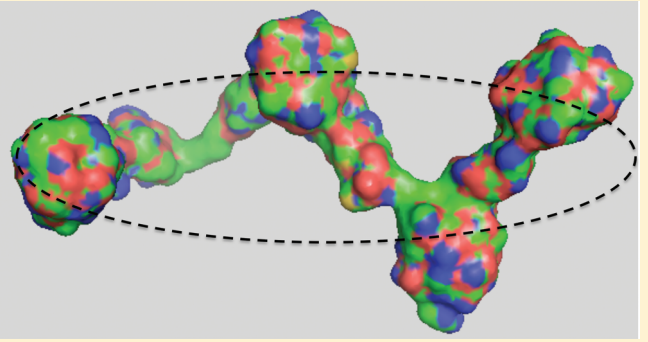

1. INTRODUCTION

Agrin is an important extracellular matrix proteoglycan that induces acetylcholine receptor aggregation at the neuromuscular junction.[1,2] The low-density lipoprotein receptor-related protein acts as a receptor for agrin and is essential for muscle-specific kinase signaling and ultimately for aggregation of the acetylcholine receptor.[3] Investigations for new functions and binding partners for agrin over the past 25 years have established its involvement in the generation and maintenance of synapses at the neuromuscular junction, immunological synapses, and synapses in the brain.[4−8]

Agrin comprises an N-terminal domain, which is followed by a series of follistatin-like domains (FS), laminin EG-like domains (LE), a serine- and threonine-rich region (S/T), a sperm protein-enterokinase-agrin domain (SEA), epidermal growth factor-like domains (EGF), and three laminin G-like domains (G1, G2, G3) at the C-terminus.[5−10] Alternative mRNA splicing has the potential to generate different forms of agrin where the presence or absence of these insertions has been related to the functional specificity of the agrin splice variants.[8,11] For example, the G2 domain has a splicing site, "A", which can form either A0 or A4 variants depending on the absence or presence of four amino acid residues. On the other hand, the G3 domain can have B0, B8, B11, and B19 variants depending on the absence or presence of an 8, 11, or 19 amino acid residue insert.[12,13] The binding of agrin to laminin is required for its localization to the synaptic basal lamina and other basement membranes and is mediated by the N-terminal domain of agrin (NtA).[14,15] The most conspicuous function of agrin is its potential involvement in the treatment of congenital muscular dystrophy, the molecular origin of which has been traced to a mutation in the gene encoding laminin where miniagrin—a miniaturized version of agrin comprising the NtA domain and all three globular C-terminal domains (Figure 1)—has been shown to amend muscle pathology and partially control congenital muscle dystrophy.[16,17]

As part of an exploration of the solution conformation of this genetically engineered protein, miniagrin has been subjected to dynamic light scattering, analytical ultracentrifugation, and small-angle X-ray scattering (SAXS) studies. However, an impediment to that endeavor has been the observation of a discrepancy between the calculated molar mass of the polypeptide chain and that obtained by combining sedimentation and diffusion coefficients in the Svedberg equation. Evidence is presented which indicates that miniagrin is not a single macromolecular entity in solution but a mixture of oligomeric states in rapid association equilibrium.

Received: July 6, 2011
Revised: August 16, 2011
Published: August 22, 2011

Figure 1. Schematic representation of miniagrin showing the arrangement of the NtA domain, FS domain, EGF domains, and globular G1, G2, and G3 domains.

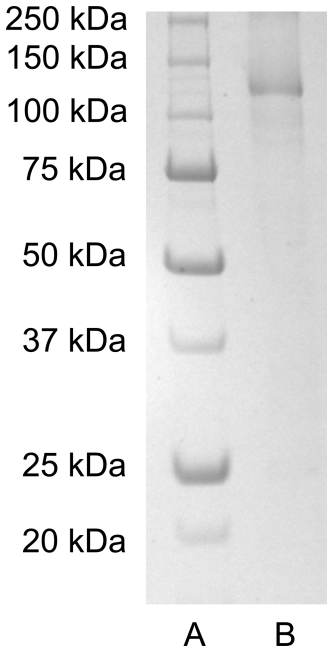

Figure 2. Check on protein purity by SDS−PAGE in tricine buffer. Lanes A and B show the standard molecular weight markers and purified miniagrin, respectively.

2. EXPERIMENTAL SECTION

2.1. Protein Expression and Purification. The miniagrin gene cloned into the pCEP-Pu plasmid was used to express the miniagrin polypeptide chain as described by Moll and coworkers.[16] HEK 293 cells were stably transfected using the nonliposomal lipid transfection reagent *Effectene* (Qiagen, California, USA) as described by the manufacturer. This step was followed by screening of transfected cells using puromycin resistance at a concentration of 2 μg/mL. HEK 293 cells were then allowed to grow with medium containing DMEM, 10% FBS, and Penicillin/Streptomycin with 2 μg/mL of puromycin at 37 °C. The protein was purified by affinity column chromatography on the HisTrap FF crude column (GE Healthcare Life Sciences, USA) and stored at 4 °C in Tris buffer, pH 7.5, I = 0.24 M (50 mM Tris-HCl, 200 mM NaCl). A check on the purity of the miniagrin preparation by SDS−PAGE in tricine buffer[18] revealed the presence of only a single band (Figure 2, lane A). Furthermore, no post-translational modification in terms of glycosylation seems to have occurred during protein expression as judged by a test for N-glycosylation by means of the PNGaseF kit (data not shown, New England Biolabs, USA). Concentrations of the purified miniagrin were determined on the basis of a molar extinction coefficient of 86 980 M^{-1} cm^{-1} that was calculated from the amino acid sequence by means of the ProtParam tool available on the ExPASy server.[19]

2.2. Dynamic Light Scattering. The dynamic light scattering profile for miniagrin was measured by means of the Zetasizer Nano S system (Malvern Instruments Ltd., Malvern, UK) equipped with a 4 mW laser (λ = 633 nm) as described earlier.[20] A scattering angle close to the direction of the incident beam was used to minimize complications through rotational diffusion behavior.[21] A stock solution of miniagrin in Tris buffer, pH 7.5, I = 0.24 M (50 mM Tris-HCl, 200 mM NaCl), was subjected to centrifugal filtration through a 0.1 μm filter (Millipore) before dilution to yield a series of solutions with concentrations in the range of 0.2−1.0 mg/mL. These solutions were allowed to equilibrate for 4 min at 20.0 °C prior to DLS measurements at the same temperature. Multiple records of the DLS profile at each protein concentration were analyzed by means of the DTS software supplied by the manufacturer (version 5.10.2, Malvern Instruments Ltd., Malvern, UK). The obtained diffusion coefficient was corrected to standard solvent conditions ($D_{20,w}$) and extrapolated to infinite dilution.

2.3. Analytical Ultracentrifugation. Sedimentation velocity experiments were performed on an Optima XL-I analytical ultracentrifuge (Beckman−Coulter, Palo Alto, CA) fitted with an An60-Ti rotor. Standard 12 mm double sector cells were loaded with 380 μL of miniagrin solution (0.15−1.2 mg/mL) in Tris buffer, pH 7.5, I = 0.24 M (50 mM Tris-HCl, 200 mM NaCl), and 400 μL of buffer in the appropriate channels. The solutions were subjected to centrifugation at 40 000 rpm and 20 °C and solute distributions at 10 min intervals recorded at 280 nm by means of the absorption optical system. The absorbance distributions were analyzed by the SEDFIT program[22,23] to obtain the weight average sedimentation coefficient $s_{20,b}$, which was then corrected to standard solvent conditions ($s_{20,w}$) using SEDNTERP,[24] and the partial specific volume of 0.727 mL/g that was obtained from the amino acid sequence of the miniagrin polypeptide chain.

For sedimentation equilibrium (SE) studies, a solution of miniagrin (0.3 mg/mL) was centrifuged at 20 000 rpm, a speed sufficient to ensure experiments of the meniscus-depletion design.[25] The resulting SE distribution was recorded by the Rayleigh interference optical system and converted to the corresponding weight−concentration distribution on the basis of a calibration factor of 3.33 fringes for a 1 mg/mL protein solution in a 12 mm cell.[26]

2.4. Small-Angle X-ray Scattering (SAXS). SAXS data were collected on 2, 3, and 4 mg/mL solutions of miniagrin in Tris buffer, pH 7.5, I = 0.24 M (50 mM Tris-HCl, 200 mM NaCl), using a Rigaku 3-pinhole camera (S-MAX3000) equipped with a Rigaku MicroMax+002 microfocus sealed tube (Cu Kα radiation at 1.54 Å) and a Confocal Max-Flux (CMF) optics system operating at 40 W (Rigaku, USA). Scattering data were recorded using a 200 mm multiwire 2D detector. The data for miniagrin were

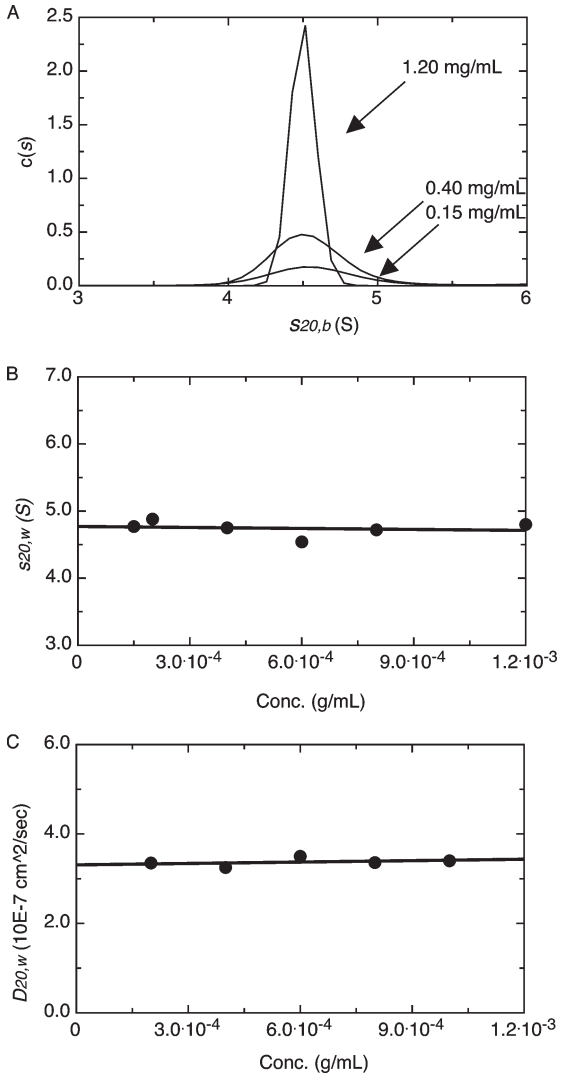

Figure 3. Hydrodynamic characterization of miniagrin (pH 7.5, I = 0.24 M). (A) Profiles obtained by $c(s)$ analysis[22,23] of sedimentation velocity distributions for the indicated concentrations of miniagrin. (B) Resultant concentration dependence of the sedimentation coefficient. (C) Concentration dependence of the translational diffusion coefficient obtained by DLS.

collected for 2 h within the range of $0.008 \leq q \leq 0.275$ Å^{-1}, where the scattering vector $q = [4\pi(\sin\theta)]/\lambda$ describes the scattering at angle 2θ of the X-ray beam with wavelength λ. Data were processed as described previously.[27] Briefly, SAXS data reduction at individual concentrations was performed using SAXGUI data processing software (Rigaku, USA) followed by subtraction of scattering data for buffer. As a check on possible radiation damage, the DLS profile of a 4 mg/mL miniagrin solution subjected to the 2 h of radiation was compared with the corresponding pattern for unirradiated protein.

SAXS data for miniagrin were also analyzed by means of the BUNCH software[28] that allows the construction of a model of the overall shape of the protein by combining high-resolution data (if available) with ab initio calculations for the domains for which the high-resolution data are missing as described earlier.[27] We used high-resolution information from PDB files 1JB3[9] for NtA, 1BMO[29] for FS, 3H5C[30] for EGF1, 3PVE (Sampathkumar, P., unpublished data) for LG1 and LG2, 2VJ3[31] for EGF2 and EGF3, and 1PZ9[7] for LG3. The homology models for FS, EGF domains, and the LG1 domain were constructed using a SWISS-MODEL server.[32]

3. RESULTS

3.1. Hydrodynamic Studies. Analyses of sedimentation velocity distributions for miniagrin at concentrations of 0.15, 0.4, and 1.2 mg/mL in Tris buffer, pH 7.5, I = 0.24 M (50 mM Tris-HCl, 200 mM NaCl), by the SEDFIT $c(s)$ procedure[22,23] are presented in Figure 3A, which signify essential concentration independence of the sedimentation coefficient over the extremely narrow protein concentration range (0.15−1.2 mg/mL) that has been examined. Such insensitivity of the sedimentation coefficient to miniagrin concentration is reinforced in Figure 3B, which summarizes the results of all runs and yields a sedimentation coefficient $s_{20,w}$ (corrected to standard conditions—a solvent with the density and viscosity characteristics of water at 20 °C) of 4.7 (±0.2) S, where the uncertainty is expressed as twice the standard deviation of the mean.

Dynamic light scattering experiments on miniagrin solutions over a narrow concentration range (0.2−1.0 mg/mL) in the same buffer yielded indistinguishable estimates of the Stokes radius (R_h) and hence, as is evident from Figure 3C, concentration independence of the translational diffusion coefficient ($D_{20,w}$) evaluated from the Stokes radius (inferred from the peak of the distribution) via the Stokes−Einstein equation

$$D_{20,w} = \frac{RT}{6\pi L \eta_{20,w} R_h} \quad (1)$$

where $\eta_{20,w}$ is the viscosity of water at 20 °C, T the absolute temperature, R the universal gas constant, and L Avogadro's number. A diffusion coefficient of 3.3 (±0.2) × 10^7 cm^2/s was obtained. An estimate of 127 000 (±12 000) g/mol was then deduced for the apparent molecular mass (M^{app}) of miniagrin by substituting the $s_{20,w}$ and $D_{20,w}$ values into the Svedberg equation

$$M^{app} = s_{20,w}\frac{RT}{D_{20,w}(1-\bar{v}\rho)} \quad (2)$$

in which $\bar{v}$ denotes the partial specific volume of the protein (0.727 mL/g) and $\rho_{20,w}$ the density of water at 20 °C.

Although the findings presented in Figure 3 are seemingly consistent with the concept of the protein being a single macromolecular entity, there is a marked disparity between the above hydrodynamic estimate of molecular mass and that of 106 650 g/mol that emanates from the amino acid sequence of the miniagrin polypeptide chain. Determination of the light scattering second virial coefficient (A_2) from SAXS data has shed light on the likely source of the discrepancy.

3.2. Evaluation of the Light Scattering Second Virial Coefficient. The deduction of structural information from the angular dependence of SAXS is conditional upon allowance for the consequences of thermodynamic nonideality via the solution structure factor $S(q)$ pertaining to a scattering vector q defined as $q = (4\pi/\lambda)\sin(\theta/2)$, where θ is the scattering angle and λ the X-ray wavelength (1.54 Å in the present study). Although $S(q)$ is usually calculated on the basis that nonideality is described by B_{22}, the osmotic second virial coefficient for protein self-interaction,[33−35] the second virial coefficient obtained by light scattering techniques also contains contributions to nonideality arising

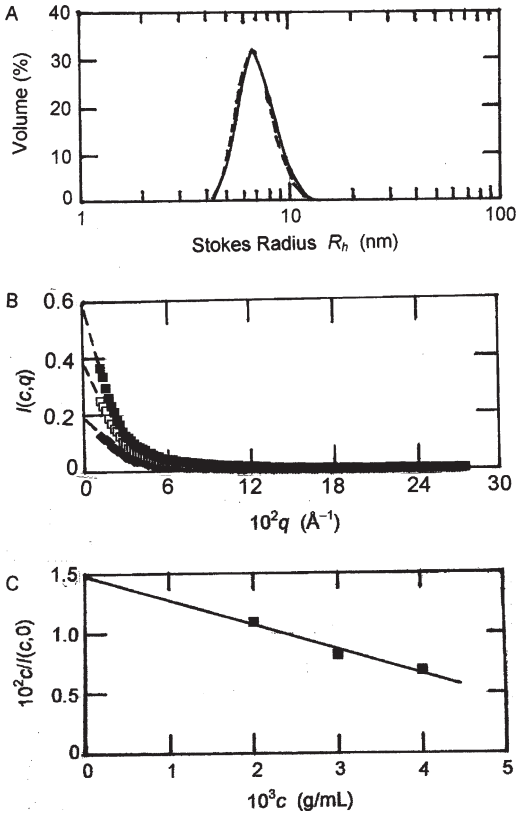

Figure 4. Evaluation of the X-ray scattering second virial coefficient. (A) Demonstration of the essential identity of DLS profiles for miniagrin (4 g/L) before (——) and after (– – –) X-ray irradiation to generate the SAXS data. (B) Extrapolation of SAXS data for miniagrin solutions (pH 7.5, I = 0.24 M) to obtain the limiting scattering intensity, $I(c,0)$, for concentrations (c) of 4 (■), 3 (□), and 2 (▲) g/L. (C) Plot of the $I(c,0)$ values in accordance with eq 3 to obtain the second virial coefficient A_2.

from protein−buffer interactions.[36−38] Fortunately, the SAXS data collected for deducing solution conformation also provides a means of determining the light scattering second virial coefficient A_2 from the concentration dependence of $S(c,0)$, the ratio of the normalized scattering intensity at zero angle for a solution with concentration c, $I(c,0)$, to that $[I(0,0)]$ at zero concentration as well as zero angle.[39−41] Specifically, results were analyzed in terms of the expression

$$\frac{c}{I(c,0)} = I(0,0) + 2I(0,0)A_2Mc + \ldots \quad (3)$$

to obtain the constant parameters A_2 and $I(0,0)$ from the linear dependence of $c/I(c,0)$ upon protein concentration. In that regard, the determination of essentially identical dynamic light scattering profiles for unirradiated miniagrin and a sample exposed for 2 h to X-rays (Figure 4A) precludes the possibility that significant structural damage to the protein may have occurred during the SAXS experiments.

The angular dependence of normalized scattering intensity $I(c,q)$ is summarized in Figure 4B, where broken lines denote the extrapolations entailed in deducing $I(c,0)$ from an assumed linear dependence in the very low angle region ($q \leq 0.02$ Å^{-1}) for miniagrin concentrations of 2 (♦), 3 (□), and 4 (■) mg/mL. A plot of those extrapolated values in accordance with the above expression (Figure 4C) is characterized by an ordinate intercept $[I(0,0)]$ of 0.0148 (±0.0014) and a slope $[2I(0,0)A_2M]$ of −2.05 (±0.48). We then obtain a light scattering second virial coefficient (A_2) of −6.5 (±1.5) × 10^{-4} mL mol g^{-2} by taking M to be 106 650 g/mol, the molecular mass calculated from the amino acid sequence of miniagrin. On the grounds that the return of a negative value of A_2 signifies that thermodynamic nonideality is giving rise to a net attractive force between miniagrin molecules, we now need to distinguish between protein self-association and protein−buffer interactions as the source of the negative value for the light scattering second virial coefficient.

3.3. Rationalization of the Hydrodynamic and SAXS Findings. As noted above, the apparent molecular mass deduced from the hydrodynamic studies exceeds by about 20% the value calculated from the amino acid sequence of miniagrin. In hydrodynamic studies, the effect of physical interaction between solute molecules leads to concentration dependences of sedimentation and diffusion coefficients for a nonassociating globular protein that are described in terms of their limiting values (s^0, D^0) by the relationships (valid for dilute solutions)

$$s = s^0(1 - k_sc) \quad (4a)$$

$$D = D^0(1 + k_Dc) \quad (4b)$$

where the concentration coefficient for s (k_s) greatly exceeds the magnitude of its diffusional counterpart, k_D. In any event, the combination of these expressions with the Svedberg equation (eq 2) shows that, to a reasonable approximation

$$M^{app} = M[1 - (k_s + k_D)c + \ldots] \quad (5)$$

whereupon the predicted effect of physical interactions between identical protein molecules in hydrodynamic experiments is the return of an apparent molecular mass that underestimates the true value. For a single macromolecular entity, the larger magnitude of the experimental molecular mass estimate would therefore imply substantial decoration of the miniagrin polypeptide chain, but that possibility is seemingly eliminated by the inability to detect any glycosylation on miniagrin.

In a thermodynamic study such as sedimentation equilibrium or X-ray scattering, the corresponding relationship is

$$M^{app} = \frac{M}{1 + 2A_2Mc + \ldots} \quad (6)$$

which again predicts underestimation of M in situations where B_{22}, the osmotic second virial coefficient for self-interaction of a single macromolecular entity (necessarily positive), dominates the magnitude of A_2. However, the light scattering second virial coefficient for miniagrin is negative, in which case the result of molar mass determination by static light scattering would be an overestimation of M. Although molar mass is, unfortunately, not a parameter to emanate from SAXS measurements, we can still employ eq 6 to ascertain the likely extent of molecular mass overestimation. Incorporation of the values of 106 650 g/mol and −6.5 × 10^{-4} mL mol g^{-2} for M and A_2, respectively, leads to an estimate of 124 000 g/mol for the apparent molecular mass of a 1 mg/mL (0.001 g/mL) solution of miniagrin. There is thus substantial agreement between the estimate of apparent molecular mass obtained hydrodynamically (127 000 g/mol) and that predicted on the basis of the measured light scattering second virial coefficient. On the grounds that it is therefore reasonable to preclude the negative contribution from protein−buffer interaction as the factor dominating the magnitude of A_2, we conclude

that the experimentally determined light scattering second virial coefficient is the consequence of B_{22} being negative—a situation that can only reflect self-association of the protein.

To gain some insight into the likely extent of self-association, we shall assume ideal solution behavior of the self-associating species, a reasonable approximation at the low protein concentrations under consideration. Such identification of the thermodynamic activities and concentrations of the oligomeric species, which for illustrative purposes we shall consider to be monomer and dimer, allows identification of M^{app} with the weight-average molecular mass of the mixture with total protein concentration $\bar{c}$. In other words, we are considering that the sole source of the negative light scattering second virial coefficient is reversible dimerization, which in the strictest sense is a form of nonideality for the single thermodynamic component, miniagrin. As noted elsewhere,[42,43] the division of forces responsible for the second virial coefficient into physical ("nonassociative") and chemical ("associative") interactions is a nonthermodynamic exercise.

Under those simplifying circumstances, weight−concentration of monomer (c_A) in a solution of a reversibly dimerizing solute ($2A \leftrightarrows C$) with total concentration $\bar{c}$ is related to the weight-average molecular mass ($\bar{M}$) by

$$\bar{M} = \frac{c_A M_A + (\bar{c} - c_A) M_C}{\bar{c}} \quad (7)$$

where the molecular mass of dimer (M_C) is twice that (M_A) of monomer. A weight-average mass of 125 000 g/mol for a 1 mg/mL solution of miniagrin would thus comprise 0.83 mg/mL of monomer and 0.17 mg/mL of dimer, values that would lead to an estimate of 0.25 L/g for the dimerization constant ($X_2 = c_D/c_M^2$). Definitive quantification of the self-association phenomenon by the present procedures is precluded by the inability to delineate the contribution of protein−buffer interactions to the light scattering second virial coefficient. In that regard, sedimentation equilibrium is the only technique that allows separate assessment of nonideality contributions arising from protein−buffer and protein−protein interactions[38,44,45] and hence the only technique that can provide unequivocal evidence for the existence of miniagrin self-association.

3.4. Further Evidence of Miniagrin Self-Association. For a more definitive appraisal of the possibility that miniagrin undergoes rapidly reversible self-association, the results from a sedimentation equilibrium experiment on the protein in the same buffer (Tris buffer, pH 7.5, I = 0.24 M) have been analyzed in terms of the relationships[46]

$$\bar{c}(r) = c_A(r_F)\psi_A(r) + X_2[(c_A(r_F)\psi_A(r_F)]^2 \quad (8a)$$

$$\psi_A(r) = \exp[M_A(1 - \bar{v}\rho)\omega^2(r^2 - r_F^2)/(2RT)] \quad (8b)$$

in which the total protein concentration, $\bar{c}(r)$, at radial distance r is written as the sum of the respective concentrations of monomer and dimer at that radial distance. Monomer concentration, $c_A(r)$, is expressed as the product of its value at a selected reference radial distance r_F and the exponential factor $\psi_A(r)$ (eq 8b) for a solute with molecular mass M_A and partial specific volume $\bar{v}$ subjected to ultracentrifugation at angular velocity ω and absolute temperature T in a solvent with density ρ. Although this psi analysis[46] has been designed to accommodate effects of thermodynamic nonideality, the substitution of concentrations for thermodynamic activities of the two species should be a reasonable approximation for such low protein concentrations (a maximum of 1.2 g/L).

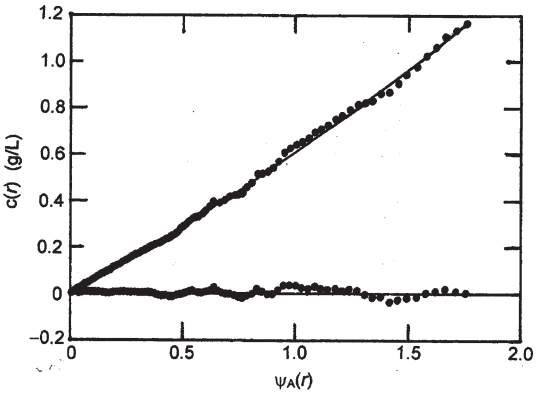

Figure 5. Analysis of the sedimentation equilibrium distribution for a 0.3 g/L solution of miniagrin (pH 7.5, I = 0.24 M) in accordance with eqs 8a and 8b to obtain a dimerization constant by nonlinear least-squares curve fitting: the essentially horizontal data set denotes the residuals plot.

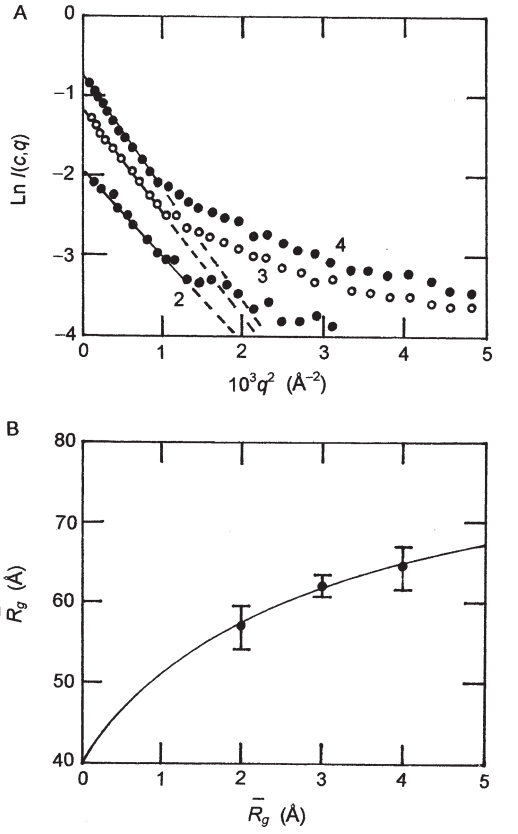

Figure 6. Analysis of SAXS data for miniagrin (pH 7.5, I = 0.24 M). (A) Guinier plots for the indicated miniagrin concentrations (g/L) showing the linear slopes used to obtain the radius of gyration from eq 9. (B) Concentration dependence of the radius of gyration and its description (——) in terms of reversible dimerization (X_2 = 0.24 L g^{-1}) and values of 40 and 105 Å for the respective radii of gyration for monomer and dimer.

Analysis of the sedimentation equilibrium distribution on the basis of a selected reference radial distance r_F of 7.15 cm and the

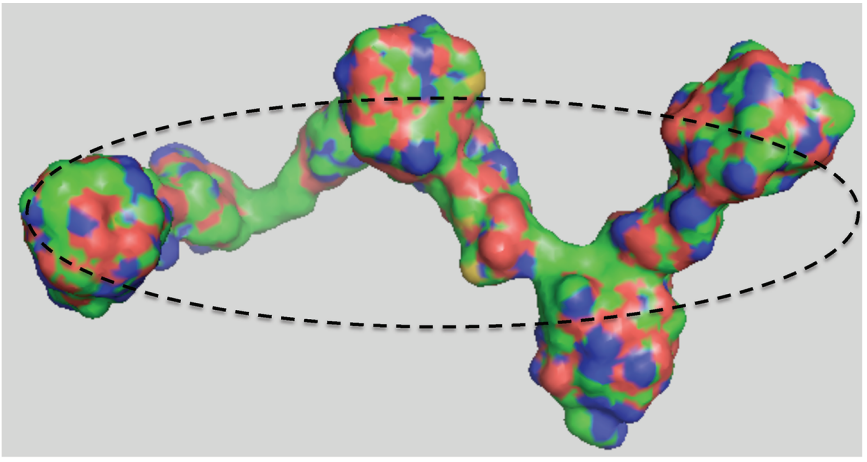

Figure 7. Comparison of the BUNCH Homology model of miniagrin monomer with its approximate representation as a prolate ellipsoid of revolution based on the radius of gyration deduced from the ordinate intercept of Figure 6 (see text).

analytical value of 106 650 g/mol for M_A yields the dependence of $\bar{c}(r)$ upon $\psi_A(r)$ shown in Figure 5, where the solid line represents the best-fit description [$c_A(r_F) = 0.538$ ($\pm$0.002) g/L, $X_2 = 0.24$ ($\pm$0.02) L/g] obtained by nonlinear least-squares curve-fitting of the data to the above equations. Although the magnitude of the tentative association constant deduced above for the putative dimerization of miniagrin is thereby confirmed, it must be stressed that Figure 5 merely attests to the adequacy of thermodynamic description in terms of the simplest stoichiometry for self-association. In other words, some form of self-association is required, but the nature of the oligomeric state in association equilibrium with monomer has not been identified unequivocally.

Additional evidence of miniagrin self-association emanates from analysis of the SAXS data [Figure 4(A)] according to the Guinier expression[47]

$$\ln I(c,q) = \ln I(0,0) - R_g^2 q^2/3 \quad (9)$$

which is normally used to evaluate the radius of gyration, R_g, of a nonassociating solute from a linear dependence of $\ln I(c,q)$ upon q^2 that is essentially independent of the protein concentration used for its determination. For miniagrin, these Guinier plots are decidedly curvilinear (Figure 6A), and the limiting slope (as $q^2 \rightarrow 0$) increases with increasing protein concentration (Figure 6B). On the grounds that the value of the radius of gyration deduced from the limiting slope ($\overline{R}_g$) would be a weight-average parameter for a reversibly dimerizing system, the expression

$$\overline{R}_g = \frac{c_A(R_g)_A + X_2 c_A^2 (R_g)_C}{\bar{c}} \quad (10)$$

has been used to evaluate values of the radius of gyration for monomer, $(R_g)_A$, and dimer, $(R_g)_C$, by solving the simultaneous equations generated by the three $[\bar{c},\overline{R}_g]$ data points . The solid line in Figure 6B signifies the concentration dependence of $\overline{R}_g$ predicted on the basis of the respective estimates of 40 ($\pm$6) and 105 ($\pm$12) Å for the radii of gyration of monomer and dimer that are obtained by pairwise combination of the three data points. The concentration dependence of the measured radius of gyration thus finds rational explanation in terms of miniagrin self-association, provided that the estimates of the radii of gyration are seemingly reasonable.

On the basis of the relationship between R_g and R_h for spherical particles, $R_g/R_h = \sqrt{(3/5)}$, the Stokes radius of a miniagrin monomer with $R_g = 4.0$ nm would be 5.16 nm, which indicates an effective hydrodynamic molar volume, $V_A = (4/3)\pi L R_A^3$, of 346 000 mL. However, the relatively small sedimentation coefficient (<4.7 S) for a 100 kDa protein signifies a markedly asymmetric shape—a feature of more detailed structural considerations (BUNCH,[28] HYDROPRO[48]), which yield an elongated molecule with a maximum length of 25 nm for monomer. By modeling the monomer as a prolate ellipsoid of revolution with respective semimajor and semiminor axes a and b, the estimate of the latter (b) for a prolate ellipsoid with volume $V_A = (4/3)\pi L a b^2$ and semimajor axis $a = 12.5$ nm (half the maximum length) is 3.3 nm. An axial ratio (a/b) of 3.8 is thus predicted for the putative monomeric species inferred from analysis of the SAXS data (Figure 6). The fact that this approximate description equates reasonably well with the BUNCH Homology Model (Figure 7) supports acceptance of the ordinate intercept of Figure 6 as the radius of gyration for monomeric miniagrin.[49]

The estimate of 10.5 nm for $(R_g)_C$ is more difficult to rationalize. At first sight, the ratio of 2.6 for $(R_g)_C/(R_g)_A$ seemingly signifies a requirement for a higher stoichiometry of self-association, but consideration of the SAXS results (Figure 6) in terms of oligomers larger than dimer leads to poorer definition of magnitudes for $(R_g)_A$ and $(R_g)_C$. An alternative source of a large $(R_g)_C$ could well be end-to-end association, whereupon the approximate description in terms of prolate ellipsoids of revolution becomes less acceptable. Side-by-side association seems precluded in that oligomerization would lead to greater asymmetry and hence smaller radii of gyration. Clearly, more extensive experimental delineation of the concentration dependence of $\overline{R}_g$ would allow better definition of $(R_g)_C$ and hence an opportunity for identifying the oligomeric state involved in the reversible self-association of miniagrin.

4. DISCUSSION

An important feature to emerge from the present hydrodynamic and thermodynamic studies of the solution behavior of miniagrin is the demonstration that this genetically engineered protein should not be regarded as a single macromolecular entity but rather as a mixture comprising monomer and oligomer(s) in

rapid association equilibrium. For illustrative purposes, the self-association equilibrium has been characterized in terms of reversible dimerization and an association constant of 0.25 L/g, which suffices to signify the presence of significant and changing proportions of the miniagrin oligomer in the concentration range 0.5−5 g/L. Such propensity for intermolecular noncovalent interaction possibly reflects a characteristic of agrin, the proteoglycan of which miniagrin is a miniaturized version, which undergoes complex formation with low-density lipoprotein receptor protein as a prerequisite for its role in muscle-specific kinase signaling and hence aggregation of the acetylcholine receptor.[3,49] On the other hand, the miniagrin self-association may well involve regions of the polypeptide chain that would normally be either involved in or masked by glycosidic decoration of the functional proteoglycan. Consequently, although the present detection of miniagrin self-association may well have important implications in future studies of events at the extracellular matrix, it will first be necessary to eliminate the possibility that the self-association merely reflects a lack of glycosidic residues on the genetically engineered protein. In either event, the present findings represent an important development in the quest for an understanding of extracellular signaling at the molecular level. Furthermore, there is the potential role of miniagrin in the control of congenital muscular dystrophy[16,17] to consider.

Miniagrin shows promise as a potential therapeutic in the treatment of congenital muscular dystrophy by gene therapy in that partial control has been achieved by injecting the miniagrin gene into mouse models.[16,17] However, although the more recent study[17] indicates a need to curtail the size of the recombinant construct for miniagrin to become a protein therapeutic for the treatment of congenital muscular dystrophy, there are potential problems with decreasing the size of the construct. First, the length of the miniagrin protein is very important for the therapeutic treatment because miniagrin connects the muscle basement membranes with dystroglycan−glycoprotein complexes. A decrease in length of the miniagrin polypeptide chain should not affect the interaction with α-dystroglycan via its G2 and G3 domains but may well preclude simultaneous binding to the basement membrane. A second potential problem confronting the use of miniagrin as a protein therapeutic is its processing and cleavage by matrix metalloproteinases (studies in progress). Nevertheless, this, potential of miniagrin for the treatment of congenital muscular dystrophy by miniagrin-linked gene-therapy certainly merits further investigation.

AUTHOR INFORMATION

Corresponding Author

*E-mail patelt@cc.umanitoba.ca. Tel.: + 1 204 4747172. Fax: +1 204 4747608.

ACKNOWLEDGMENT

TRP thanks the Canadian Institutes of Health Research for the award of a Postdoctoral Fellowship. J.S., who holds the Canada Research Chair in Structural Biology, also acknowledges the Canadian Institutes of Health Research for funding support on the agrin project. Professor Markus Ruegg kindly provided the minagrin gene.

REFERENCES

(1) Nitkin, R. M.; Smith, M. A.; Magill, C.; Fallon, J. R.; Yao, Y. M.; Wallace, B. G.; McMahan, U. J. *J. Cell Biol.* **1987**, *105*, 2471.
(2) Wallace, B. G. *J. Neurosci.* **1989**, *9*, 1294.
(3) Kim, N.; Stiegler, A. L.; Cameron, T. O.; Hallock, P. T.; Gomez, A. M.; Huang, J. H.; Hubbard, S. R.; Dustin, M. L.; Burden, S. J. *Cell* **2008**, *135*, 334.
(4) Fallon, J. R.; Nitkin, R. M.; Reist, N. E.; Wallace, B. G.; McMahan, U. J. *Nature* **1985**, *315*, 571.
(5) Rupp, F.; Payan, D. G.; Magill-Solc, C.; Cowan, D. M.; Scheller, R. H. *Neuron* **1991**, *6*, 811.
(6) Tsen, G.; Napier, A.; Halfter, W.; Cole, G. J. *J. Biol. Chem.* **1995**, *270*, 15934.
(7) Stetefeld, J.; Alexandrescu, A. T.; Maciejewski, M. W.; Jenny, M.; Rathgeb-Szabo, K.; Schulthess, T.; Landwehr, R.; Frank, S.; Ruegg, M. A.; Kammerer, R. A. *Structure* **2004**, *12*, 503.
(8) Mascarenhas, J. B.; Ruegg, M. A.; Winzen, U.; Halfter, W.; Engel, J.; Stetefeld, J. *EMBO J.* **2003**, *22*, 529.
(9) Stetefeld, J.; Jenny, M.; Schulthess, T.; Landwehr, R.; Schumacher, B.; Frank, S.; Ruegg, M. A.; Engel, J.; Kammerer, R. A. *Nat. Struct. Biol.* **2001**, *8*, 705.
(10) McFarlane, A. A.; Stetefeld, J. *Protein Sci.* **2009**, *18*, 2421.
(11) Campanelli, J. T.; Gayer, G. G.; Scheller, R. H. *Development* **1996**, *122*, 1663.
(12) O'Toole, J. J.; Deyst, K. A.; Bowe, M. A.; Nastuk, M. A.; McKechnie, B. A.; Fallon, J. R. *Proc. Natl. Acad. Sci. U.S.A.* **1996**, *93*, 7369.
(13) Stetefeld, J.; Ruegg, M. A. *Trends Biochem. Sci.* **2005**, *30*, 515.
(14) Denzer, A. J.; Brandenberger, R.; Gesemann, M.; Chiquet, M.; Ruegg, M. A. *J. Cell Biol.* **1997**, *137*, 671.
(15) Kammerer, R. A.; Schulthess, T.; Landwehr, R.; Schumacher, B.; Lustig, A.; Yurchenco, P. D.; Ruegg, M. A.; Engel, J.; Denzer, A. J. *EMBO J.* **1999**, *18*, 6762.
(16) Moll, J.; Barzaghi, P.; Lin, S.; Bezakova, G.; Lochmuller, H.; Engvall, E.; Muller, U.; Ruegg, M. A. *Nature* **2001**, *413*, 302.
(17) Meinen, S.; Barzaghi, P.; Lin, S.; Lochmuller, H.; Ruegg, M. A. *J. Cell Biol.* **2007**, *176*, 979.
(18) Schägger, H. *Nat. Protoc.* **2006**, *1*, 16.
(19) Gasteiger, E.; Hoogland, C.; Gattiker, A.; Duvaud, S.; Wilkins, M. R.; Appel, R. D.; Bairoch, A. Protein Identification and Analysis Tools on the ExPASy Server. In *The Proteomics Protocols Handbook*; Walker, J. M., Ed.; Humana Press: New York, 2005; p 571.
(20) Patel, T. R.; Meier, M.; Li, J.; Morris, G.; Rowe, A. J.; Stetefeld, J. *Protein Sci.* **2011**, *20*, 931.
(21) Harding, S. E. *Biotechnol. Appl. Biochem.* **1986**, *8*, 489.
(22) Dam, J.; Schuck, P. *Numer. Comput. Methods, Part E* **2004**, 185.
(23) Schuck, P. *Biophys. J.* **1998**, *75*, 1503.
(24) Laue, T. M.; Shah, B. D.; Ridgeway, T. M.; Pelletier, S. L. Computer-aided interpretation of analytical sedimentation data for proteins. In *Analytical Ultracentrifugation in Biochemistry and Polymer Science*; Harding, S. E., Rowe, A. J., Horton, J. C., Eds.; Royal Society of Chemistry: Cambridge, United Kingdom, 1992; p 90.
(25) Yphantis, D. A. *Biochemistry* **1964**, *3*, 297.
(26) Voelker, P. *Prog. Colloid Polym. Sci.* **1995**, *99*, 162.
(27) Patel, T. R.; Morris, G. A.; Zwolanek, D.; Koch, M.; Harding, S. E.; Stetefeld, J. *Matrix Biol.* **2010**, *29*, 565.
(28) Petoukhov, M. V.; Svergun, D. I. *Biophys. J.* **2005**, *89*, 1237.
(29) Hohenester, E.; Maurer, P.; Timpl, R. *EMBO J.* **1997**, *16*, 3778.
(30) Huang, X.; Dementiev, A.; Olson, S. T.; Gettins, P. G. *J. Biol. Chem.* **2010**, *285*, 20399.
(31) Cordle, J.; Johnson, S.; Tay, J. Z.; Roversi, P.; Wilkin, M. B.; de Madrid, B. H.; Shimizu, H.; Jensen, S.; Whiteman, P.; Jin, B.; Redfield, C.; Baron, M.; Lea, S. M.; Handford, P. A. *Nat. Struct. Mol. Biol.* **2008**, *15*, 849.
(32) Arnold, K.; Bordoli, L.; Kopp, J.; Schwede, T. *Bioinformatics* **2006**, *22*, 195.
(33) Curtis, R. A.; Prausnitz, J. M.; Blanch, H. W. *Biotechnol. Bioeng.* **1998**, *57*, 11.
(34) Zhang, F.; Skoda, M. W.; Jacobs, R. M.; Martin, R. A.; Martin, C. M.; Schreiber, F. *J. Phys. Chem. B* **2007**, *111*, 251.
(35) Ianeselli, L.; Zhang, F.; Skoda, M. W.; Jacobs, R. M.; Martin, R. A.; Callow, S.; Prevost, S.; Schreiber, F. *J. Phys. Chem. B* **2010**, *114*, 3776.

(36) Kirkwood, J. G.; Goldberg, R. J. *J. Chem. Phys.* **1950**, *18*, 54.
(37) Stockmayer, W. H. *J. Chem. Phys.* **1950**, *18*, 58.
(38) Winzor, D. J.; Deszczynski, M.; Harding, S. E.; Wills, P. R. *Biophys. Chem.* **2007**, *128*, 46.
(39) Receveur, V.; Durand, D.; Desmadril, M.; Calmettes, P. *FEBS Lett.* **1998**, *426*, 57.
(40) Bonneté, F.; Vivarès, D.; Robert, C.; Colloc'h, N. *J. Cryst. Growth* **2001**, *232*, 330.
(41) Vivarès, D.; Bonneté, F. *Acta Crystallogr., Sect. D: Biol. Crystallogr.* **2002**, *58*, 472.
(42) Hill, T. L.; Chen, Y.-D. *Biopolymers* **1973**, *12*, 1285.
(43) Wills, P. R.; Jacobsen, M. P.; Winzor, D. J. *Biophys. J.* **2000**, *79*, 2178.
(44) Jacobsen, M. P.; Wills, P. R.; Winzor, D. J. *Biochemistry* **1996**, *35*, 13173.
(45) Deszczynski, M.; Harding, S. E.; Winzor, D. J. *Biophys. Chem.* **2006**, *120*, 106.
(46) Wills, P. R.; Jacobsen, J. P.; Winzor, D. J. *Biopolymers* **1996**, *38*, 119.
(47) Guinier, A.; Fourner, G. *Small angle scattering of X-rays*; Wiley: New York, 1955.
(48) GarcÌa de la Torre, J.; Huertas, M. L.; Carrasco, B. *Biophys. J.* **2000**, *78*, 719.
(49) Zhang, B.; Luo, S.; Wang, Q.; Suzuki, T.; Xiong, W. C.; Mei, L. *Neuron* **2008**, *60*, 285.